



23 **One sentence summary (200 characters max):**

24 A simple method allows calculation of apoplast hydration and efficient extraction of apoplast  
25 contents from maize seedling leaves.

26 **List of Author Contributions:**

27 I.G. and D.M. designed the experiments and analyzed data; I.G., L.G., and W.Z. performed the  
28 experiments; D.M and A.A. supervised the experiments; and I.G. wrote the paper with  
29 contributions from all the authors.

30 **Funding information:**

31 This work was funded by the US Department of Agriculture (National Institute of Food and  
32 Agriculture, grant #2015-11870612), the Korean Rural Development Administration  
33 Next-Generation BioGreen 21 Program (System and Synthetic Agro-  
34 Biotech Center, PJ01326904) and the Center for Applied Plant Sciences at The Ohio State  
35 University. I.G. was supported by a USDA AFRI-ELI predoctoral fellowship (award 2017-67011-  
36 26080) and by the Translational Plant Sciences graduate program.

37 **Present addresses:**

38 **Corresponding author email**

39 Address correspondence to [mackey.86@osu.edu](mailto:mackey.86@osu.edu)

40

41

42

43

44

45 **Abstract:**

46           The plant leaf apoplast is a dynamic environment subject to a variety of both internal  
47 and external stimuli. In addition to being a conduit for water vapor and gas exchange involved  
48 in transpiration and photosynthesis, the apoplast also accumulates many nutrients transported  
49 from the soil as well as those produced through photosynthesis. The internal leaf also provides  
50 a protective environment for endophytic and pathogenic microbes alike. Given the diverse  
51 array of physiological processes occurring in the apoplast, it is expedient to develop methods to  
52 study its contents. Many established methods rely on vacuum infiltration of an apoplast wash  
53 solution followed by centrifugation. In this study, we describe a refined method optimized for  
54 maize (*Zea mays*) seedling leaves, which not only provides a simple procedure for obtaining  
55 apoplast fluid, but also allows direct calculation of apoplast hydration at the time of harvest for  
56 every sample. In addition, we describe an abbreviated method for estimating apoplast  
57 hydration if the full apoplast extraction is not necessary. Finally, we show the applicability of  
58 this optimized apoplast extraction procedure for plants infected with the maize pathogen  
59 *Pantoea stewartii* subsp. *stewartii*, including the efficient isolation of bacteria previously  
60 residing in the apoplast. The approaches to establishing this method should make it generally  
61 applicable to other types of plants.

62 **Introduction:**

63           The leaf apoplast plays key physiological roles in plants. Leaves consist of an outer  
64 epidermal cell layer that confines the inner mesophyll and vasculature tissues. Far from a solid  
65 mass of cells, the interior of the leaf has extracellular spaces, collectively known as the  
66 apoplast, that are filled with air, liquid, and cell wall material (Sattelmacher, 2000). This open

67 region of the leaf plays a vital role in the day-to-day physiology of the plant, including  
68 transpiration and photosynthesis. Water transport to the shoot is maintained by transpiration;  
69 thus, water originating at the roots ultimately arrives in the apoplast prior to water vapor  
70 release through stomata (Sattelmacher, 2000; Lawson et al., 2014). Stomata also facilitate the  
71 introduction of environmental carbon dioxide into the internal leaf, where it is then consumed  
72 during photosynthesis (Lawson et al., 2014). The apoplast further acts as a conduit in the  
73 transport of photosynthetically derived sucrose during the phloem-loading process (Geiger et  
74 al., 1974; Giaquinta, 1977; Zhang and Turgeon, 2018). Amino acid trafficking to the phloem also  
75 requires apoplastic transport (Koch et al., 2003; Lalonde et al., 2003; Zhang and Turgeon, 2018).  
76 Finally, specialized metabolism is closely linked with the apoplast during the biosynthesis of cell  
77 wall material, especially the deposition of lignins (Liu et al., 2018).

78 Abiotic stresses such as drought, soil contamination, and light quality can all affect the  
79 physiological processes occurring in the leaf apoplast. Decreasing soil moisture has been shown  
80 to increase the pH in tomato leaf apoplast (Jia and Davies, 2007; Geilfus, 2017), which in turn  
81 can impact the activity of apoplast-exposed, pH-sensitive transporters (Rottmann et al., 2018).  
82 The elemental composition of soil also has a direct impact on the leaf apoplast. Calcium, an  
83 essential plant nutrient, is absorbed by the roots and deposited into the apoplast prior to being  
84 transported into leaf cells (Wang et al., 2017). Silicon, one of the most abundant elements in  
85 the Earth's crust, is also deposited in the apoplast, where it is known to confer some nutrient  
86 value as well as play a defensive role against invading microbes (Wang et al., 2013; Wang et al.,  
87 2017; Coskun et al., 2018; Rasoolizadeh et al., 2018). Silicon can also alleviate the toxicity of  
88 excess manganese, another plant nutrient that accumulates in the apoplast (Führs et al., 2009).

89           Physiological roles aside, the apoplast also serves as a niche for endophytic microbes.  
90   These organisms, which tend to be present at low levels, maintain a presence that can actually  
91   benefit the plant, much as soil microbes offer benefits in the rhizosphere (Kandel et al., 2017).  
92   These populations are kept at bay through the plant immune system, including the ability of the  
93   plant to control water availability in the apoplast (Xin et al., 2016; Wright and Beattie, 2004).  
94   However, foliar pathogens overcome plant defenses to aggressively colonize the leaf apoplast,  
95   proliferate to high levels, and cause disease (Jones and Dangl, 2006; Liu et al., 2017). Many  
96   foliar pathogens elicit water-soaking in susceptible plants, during which the apoplast  
97   accumulates a higher than normal aqueous content that causes the leaf to appear translucent  
98   (Asselin et al., 2015; Xin et al., 2016; Schwartz et al., 2017). Plants and their pathogens also  
99   compete in various ways to control the availability of sugar in the apoplast, including regulation  
100   of host-derived cell wall invertases and pathogen-derived endoglucanase, pathogen-induced  
101   transcription of host SWEET family sugar transporters, and host-defense-induced activity of  
102   sucrose uptake transporters (Bonfig, et al., 2010; Yamada, et.al., 2016; Veillet, et al., 2016; Cox,  
103   et al., 2017). Thus, apoplast-localized events, including the availability of water and nutrients,  
104   as well as the mobilization of antimicrobial compounds and materials for cell wall  
105   reinforcement, are major determinants of susceptibility versus resistance in plant-bacteria  
106   interactions (Kwon, et al., 2008; Beattie, 2011; Xin, et al., 2016; Naseem, et al., 2017).

107           There have been a number of publications detailing centrifugation-based methods for  
108   extracting apoplast fluid from plant leaves (Lohaus et al., 2001; Witzel et al., 2011; Joosten,  
109   2012; Nouchi et al., 2012; O'Leary et al., 2014). Depending on the plant species and the  
110   downstream goal of the apoplast extraction, specific details of the methods vary significantly.

111 For example, some studies focus on the effects of nutrient deficiencies on the apoplast (López-  
112 Millán et al., 2000), while others optimize methods for studies with plant pathogens (Rico and  
113 Preston, 2008; Floerl et al., 2012; O'Leary et al., 2016; Schwartz et al., 2017). In this study, we  
114 improve upon several current apoplast extraction methods and optimize the procedure for  
115 maize (*Zea mays*) seedling leaves. Furthermore, we describe how to calculate leaf apoplast  
116 hydration without using dye or oil treatments that are usually included for representative  
117 samples. A simplified method for estimating apoplast hydration is also included for when  
118 isolation of apoplast contents is not needed. To illustrate the usefulness of this infiltration-  
119 centrifugation method, we describe apoplast hydration as a response to the maize pathogen  
120 *Pantoea stewartii* subsp. *stewartii* (*Pnss*) and demonstrate efficient isolation of the bacteria  
121 along with the apoplast contents.

122

123 **Results:**

124 **General procedures of the apoplast extraction method**

125           The apoplast extraction in this study targets the first true leaf tips of maize seedlings.  
126 Due to their small size, a pool of eight 4- to 5-cm-long leaf tips are harvested for each sample  
127 and processed to extract their apoplast contents, as shown in Figure 1. After recording the  
128 bulked leaves' initial weight (IW) and/or leaf area, they were placed in a 60cc syringe barrel  
129 containing the apoplast wash solution. Repeated pull-and-release vacuum cycles with the  
130 syringe facilitated the wash solution entrance into the apoplast. Once maximally saturated, the  
131 leaves were removed from the wash solution and then gently and thoroughly wiped dry prior to  
132 determining the after-infiltration weight (AIW). The leaves were then positioned on a 5x10-cm  
133 piece of Parafilm and carefully wrapped around a 1-mL pipet tip for structure. A second piece  
134 of Parafilm was added to hold the bundle together and suspended above the bottom of a 15-  
135 mL conical tube. This tube, with leaf tips down, was then centrifuged at 2,500 x g for 10  
136 minutes at 4°C. Leaves were weighed post centrifugation to obtain the after-spin weight  
137 (ASW). The apoplast liquid released from the leaves, along with any solids (*i.e.* bacteria), was  
138 then gently resuspended, transferred to a 1.5-mL microcentrifuge tube and centrifuged at 2320  
139 x g for 5 minutes at 4°C. The supernatant was then transferred to a fresh tube for subsequent  
140 analysis.

141 **Evaluation of apoplast extraction efficiency and leaf cellular integrity after the procedure**

142           To verify that the described extraction method was not introducing symplast  
143 contamination from ruptured cells, we performed three check experiments of the extraction

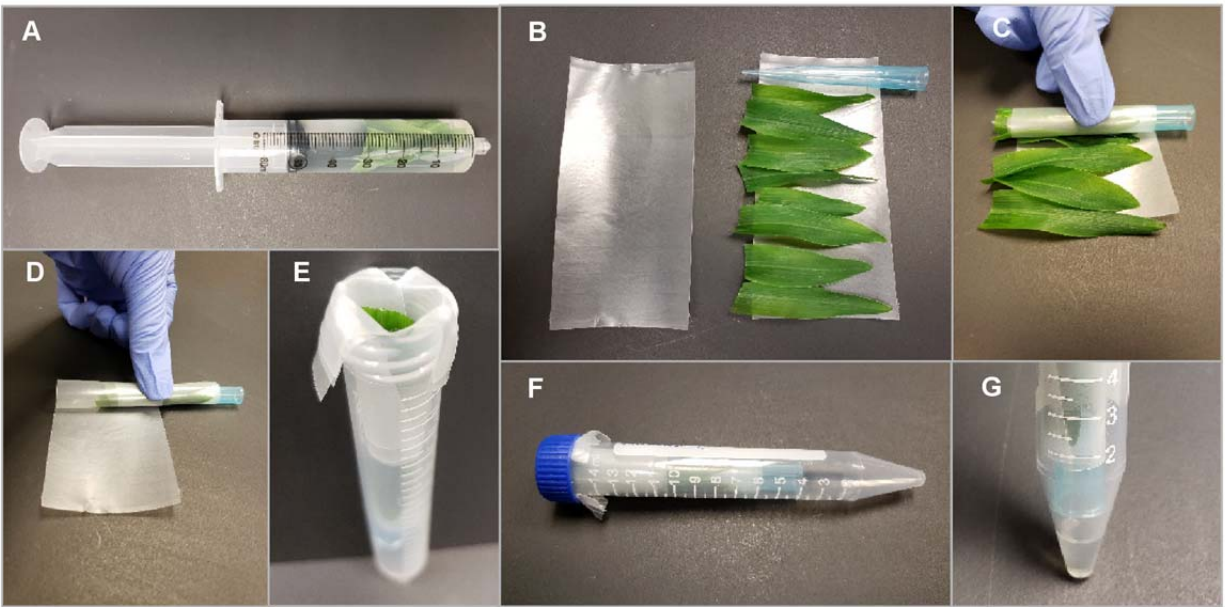


**Figure 1.** General procedure of maize leaf apoplast extraction. (A) First-true-leaf tips are harvested and syringe-infiltrated with the apoplast wash fluid. (B) The fully saturated leaves are wiped dry on their surface and placed on a 5x10 cm piece of Parafilm. A 1mL pipet tip is oriented in the opposite orientation as the leaves. (C) Keeping the leaves snug against the pipet tip, they are carefully wrapped into a cylinder. (D) To keep the bundle assembled, a second piece of Parafilm is wrapped around the leaves before inserting the bundle into a 15mL conical tube (E). The Parafilm is folded over the top of the tube before replacing the cap (F). The tube is then spun at 2,500 x g for 10 minutes at 4°C. After this step, the aqueous apoplast contents can be recovered separately from the intact leaf bundle (G). Although the leaf bundle often slides downwards during centrifugation, the size of the pipet tip ensures the bundle remains elevated above the liquid extract.

144 process. The first, shown in Figure 2A, was to determine apoplast wash solutions that maintain  
 145 cellular integrity. Water has been used as an apoplast wash solution in many studies (Lohaus et  
 146 al., 2001; Witzel et al., 2011; Joosten, 2012; O'Leary et al., 2014) and was therefore not  
 147 expected to cause any significant loss of cellular integrity. For applications intended to analyze

148 metabolites from within the apoplast, inclusion of methanol in the apoplast wash solution can  
149 increase solubility. Thus, leaves that were syringe-infiltrated with deionized water, 20%  
150 methanol, or 40% methanol were tested for cellular integrity. Following syringe-infiltration  
151 with each apoplast wash solution, the leaves were incubated in water for 1 hour prior to

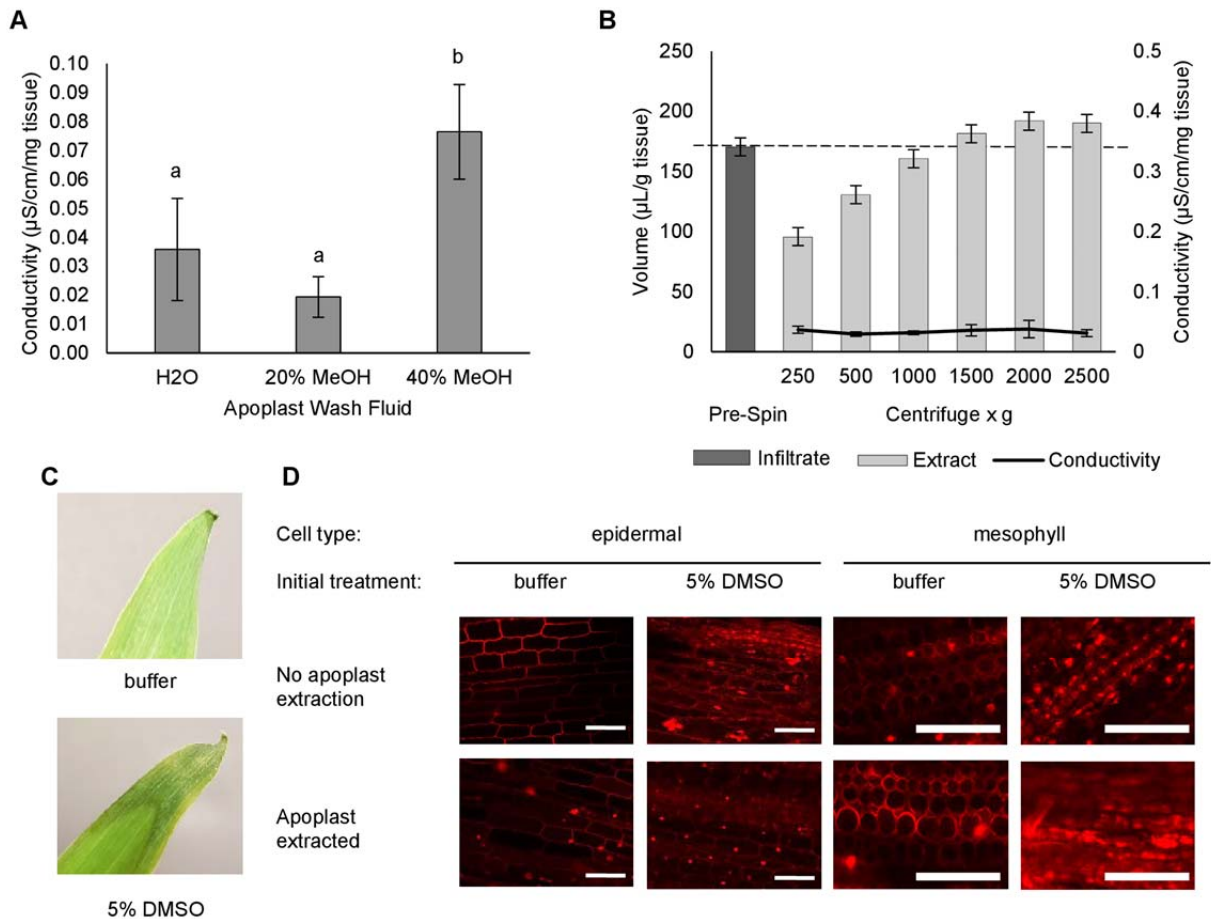


**Figure 2.** Evaluation of cellular integrity after apoplast extraction. (A) Conductivity of maize seedling leaves syringe-infiltrated with deionized water, 20% methanol, and 40% methanol. Error bars represent standard deviation of three replicates per treatment. Letters signify the significance between treatments, as assessed by one-way ANOVA followed by Tukey's HSD test where  $p \leq 0.05$ . (B) Impact of centrifugal force on the isolation of apoplast fluid from maize seedling leaves. Infiltrate represents the average volume syringe-infiltrated across all treatments. Conductivity of leaves was assessed after centrifugation. Error bars represent the standard deviation from three replicates for each treatment. (C) Representative photos of maize seedling leaf symptoms at 12 hours after vacuum-infiltration (hai) with buffer or 5% DMSO. (D) Confocal microscopic images of propidium iodide stained epidermal and mesophyll cell layers of maize leaves at 12 hai with buffer or 5% DMSO. Shown are leaves that were not (top images) or were (bottom images) subjected to the apoplast extraction procedure. Two biological replicates, each with two samples per treatment, were analyzed. Scale bars are 100  $\mu\text{m}$ .

152 measuring the conductivity of the solution. Leaves infiltrated with water or 20% methanol

153 showed similar conductivity, while 40% methanol caused a significant increase in conductivity.

154 Thus, either water or 20% methanol was deemed an appropriate apoplast wash solution.

155 Indeed, metabolite analysis revealed that 20% methanol was suitable for quantification of

156 amino acids, sugars, organic acids, phosphorylated compounds, and phenolics within a single  
157 extract volume of approximately 100  $\mu$ L from eight maize seedling leaves (unpublished data), at  
158 levels comparable to or exceeding those described in (Lohaus et al., 2001).

159         Next, the impact of centrifugation force on yield and cellular integrity was assessed  
160 (Figure 2B). The goal was to identify centrifugation conditions that provide maximal yield of  
161 apoplast contents without damaging the integrity of leaf cells. Seedling leaves were syringe-  
162 infiltrated with water and apoplast extracts collected by spinning for 10 minutes at a range of  
163 centrifugal forces from 250 x g to the instrument maximum at 2,500 x g. The volume of water  
164 infiltrated and the volume of liquid extracted were determined by the difference between leaf  
165 weight after infiltration and before infiltration or after centrifugation, respectively. It might  
166 seem intuitive to directly measure the volume of recovered liquid; however, because some  
167 liquid is retained on surfaces of the extraction apparatus, the directly measured volume was  
168 consistently less than that calculated from the difference between leaf weight after infiltration  
169 and after centrifugation. Thus, the differences in leaf weight are a more reliable measure of  
170 extraction. The volume infiltrated per leaf mass prior to the different spins was similar  
171 between samples, and the volume extracted per leaf mass increased as expected with the  
172 increase in centrifugal force. The extracted liquid exceeded the input water at 1,500 x g and  
173 plateaued at 2,000 and 2,500 x g. This indicates full recovery of both the infiltrated water and  
174 the preexisting contents of the apoplast. Conductivity measurements of leaves post  
175 centrifugation did not differ at any of the tested centrifugal forces and did not differ from those  
176 for water-infiltrated, nonextracted leaves (compare conductivity levels in Figure 2B with those  
177 in Figure 2A). Furthermore, doubling the centrifugation time at maximum speed did not

178 significantly increase ion leakage (data not shown). Therefore, to ensure quantitative yield of  
179 apoplast contents without any apparent loss of cellular integrity, we used 2,500 x g for 10  
180 minutes as the centrifugation step in this protocol.

181 Finally, confocal microscopy was used as a further check of leaf cellular integrity after  
182 the apoplast extraction process. To assess cellular damage, leaves were stained with 100  
183  $\mu\text{g}/\text{mL}$  propidium iodide (PI) for 1 hour to mark the cell walls. PI does not efficiently pass  
184 through intact plasma membranes but will stain the nuclei of damaged cells (Jones et al., 2016).  
185 It is well documented that dimethylsulfoxide (DMSO) can increase the permeability of lipid  
186 bilayers, though few studies have examined this effect in plants (Delmer, 1979; Notman et al.,  
187 2006). To generate plants with a permeable plasma membrane to mimic damaged cells, we  
188 vacuum-infiltrated maize seedlings with a solution of 0.2% Tween-40 (buffer) or also containing  
189 5% DMSO and waited 12 hours to allow DMSO-induced leaf browning symptoms to develop  
190 (Figure 2C). To visualize cellular integrity following these treatments, as well as following the  
191 apoplast extraction procedure, confocal microscopy images were collected on the adaxial side  
192 of the outermost 1-cm section of leaf tips from these seedlings prior to and post apoplast  
193 extraction (Figure 2D).

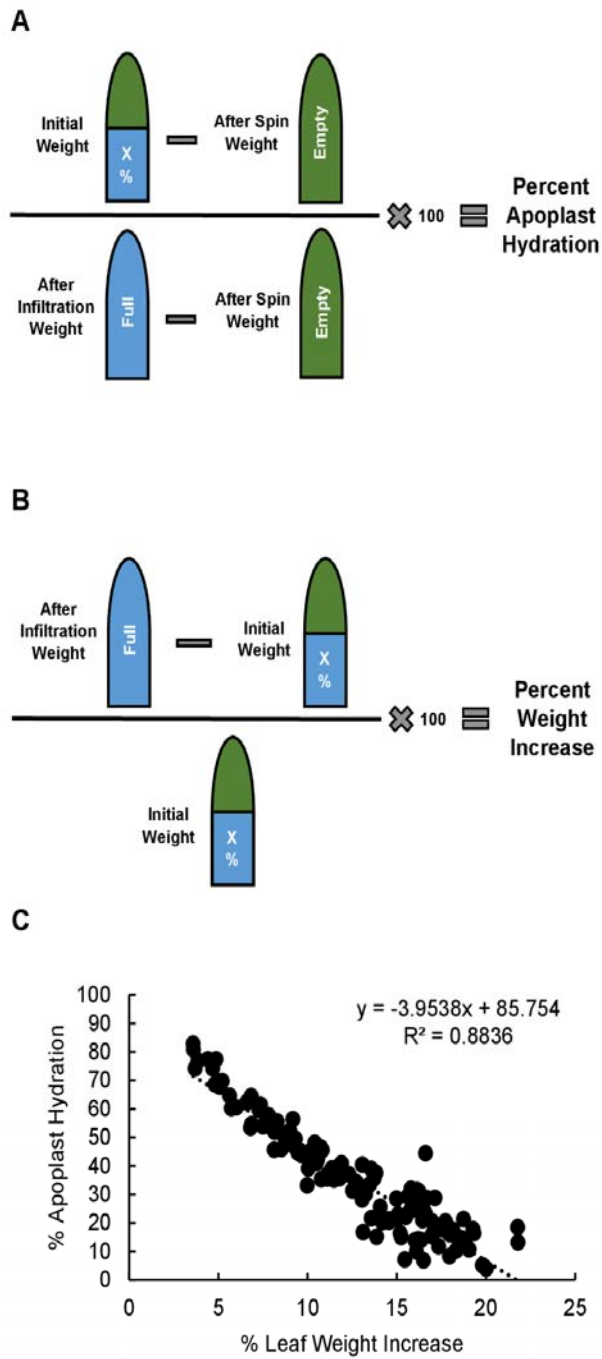
194 The status of cells from leaves treated with 5% DMSO showed a different staining  
195 pattern compared to the buffer control leaves. While the cell walls of epidermal and guard cells  
196 could easily be brought into focus on the buffer-infiltrated plants, the epidermal layer of 5%  
197 DMSO-treated leaves showed significant disorganization of cell walls and additional staining of  
198 unknown (possibly disrupted) intracellular structures. These disruptions of the epidermal layer  
199 are apparent prior to and do not significantly change after the apoplast extraction procedure.

200 Similarly, DMSO-treated mesophyll cells have nondescript cell walls and an abundance of  
201 unidentified intracellular structures both prior to and after apoplast extraction. Thus, PI  
202 staining reveals disruptions in maize cell integrity.

203 Image analysis of non-DMSO-treated leaves revealed that the well-organized PI-staining  
204 patterns of cell walls in round mesophyll cells and files of epidermal cells are unperturbed by  
205 the apoplast extraction procedure. This indicates that overall cellular integrity remains largely  
206 intact following the procedure. The PI staining of intracellular structures (presumably nuclei) is  
207 unchanged in mesophyll cells, which are the most abundant cell type, and increases only  
208 modestly in epidermal cells. Indeed, while DMSO-treated leaves displayed significant staining  
209 of epidermal nuclei before and after the apoplast extraction procedure, buffer-treated plants  
210 displayed only modest levels of stained nuclei. Analysis of several images over two replicates  
211 revealed that the background level of stained nuclei in buffer-treated leaves was 3.6-7.7%  
212 initially and increased to 9.1-11.6% following apoplast extraction (ranges from independent  
213 samples with 420 and 173 total cells counted for each analysis, respectively). Thus, the  
214 apoplast extraction procedure does not disrupt the ability of the majority of maize cells to  
215 exclude PI. Collectively, the data in this section indicate that the apoplast isolation procedure  
216 keeps cells of the maize seedling leaves largely intact.

### 217 **Calculation of apoplast hydration**

218 Understanding the extent to which the apoplast is filled with liquid, which we termed  
219 apoplast hydration, is significant to biotic stress and will likely provide useful information in the  
220 study of other developmental processes and stress responses in plants. An important aspect of

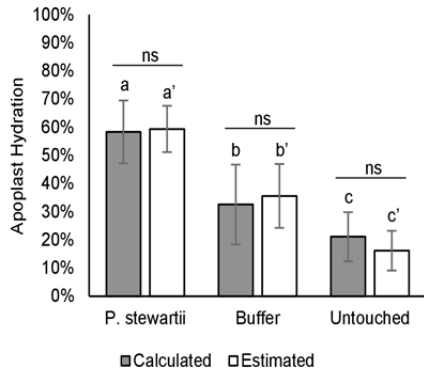
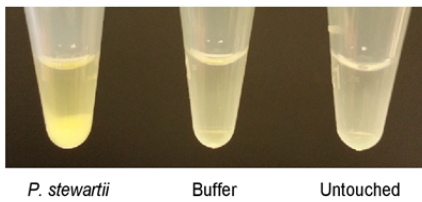
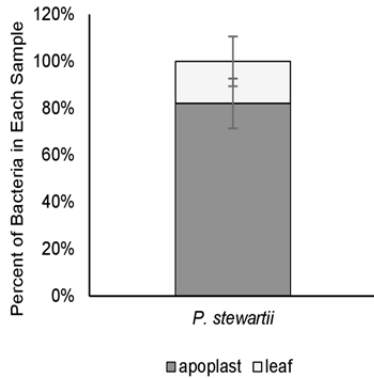


**Figure 3.** Apoplast hydration calculation. (A) Apoplast hydration can be determined using leaf weights measured during the apoplast extraction procedure. (B) Apoplast hydration also determines the percent weight increase of leaves after the syringe-infiltration step. (C) Linear correlation between apoplast hydration calculated as in (A) and percent weight increase of syringe infiltrated leaves calculated as in (B), where  $n=130$ .

221 the method we have developed is that it permits the direct calculation of apoplast hydration

222 prior to the initiation of the procedure. Specifically, apoplast hydration can be calculated from  
223 the leaf weights measured before and after the syringe-infiltration of apoplast wash solution, as  
224 well as after centrifugation (Figure 3A). At the time of collection, the apoplast has an unknown  
225 level of hydration. Based on our consistent results in Figure 2B, the apoplast is assumed to be  
226 fully hydrated after syringe infiltration with the apoplast wash solution and completely  
227 evacuated post centrifugation. Therefore, the formula  $(IW-ASW)/(AIW-ASW)$  represents the  
228 ratio of the original apoplast liquid volume and the overall capacity of the apoplast. It is  
229 imperative for experiments across plant types, age, and/or growth conditions that the  
230 extraction centrifugal force and duration (as described in Figure 2B) be optimized to ensure  
231 accurate apoplast hydration calculation using this formula.

232           For studies that are solely interested in determining apoplast hydration, it is  
233 cumbersome to repeatedly complete all steps of the apoplast extractions outlined above.  
234 Instead, after establishing the assay for a given system, an abbreviated method can be  
235 performed that provides a close estimate of apoplast hydration. This method uses the leaf  
236 weights before and after syringe-infiltration of the apoplast wash solution to calculate the  
237 percentage of weight increase of the leaves during this step (Figure 3B). Plotting the  
238 percentage of weight increase against the apoplast hydration yields a clear linear correlation  
239 (Figure 3C). The equation for this line, which would need to be independently determined for  
240 each particular system of study, can solve for apoplast hydration using only the percentage of  
241 weight increase. In our case, the equation was generated from 130 apoplast extractions from  
242 leaves that were previously untreated or were at various times after vacuum-infiltration of  
243 buffer or *P<sub>nss</sub>*. The values generated using the estimated method did not differ significantly

**A****B****C**

**Figure 4.** Application of the apoplast extraction method with a maize pathogen. (A) Apoplast hydration of maize leaves 7hai with wild-type *P. stewartii* or buffer, or leaves that were not previously infiltrated. Hydration determined with the calculated vs estimated methods yield non-significantly different values across treatments that are themselves significantly different. Significance between methods was assessed via t-test where  $p \leq 0.05$ , and significance between treatments was assessed via one-way ANOVA followed by Tukey's HSD test where  $p \leq 0.05$ . (B) Representative photos of apoplast extracts isolated from *P. stewartii*- or buffer-infiltrated plants at 12 hai compared to non-infiltrated plants. Note the large bacterial pellet in the *P. stewartii* extract. (C) Distribution of *P. stewartii* between the apoplast extract and the corresponding leaf tissue following apoplast extraction. Error bars represent standard deviation from two biological replicates where  $n=4$ .

244 from those utilizing the full apoplast extraction method, and differences in hydration also can

245 be separated on a by-treatment basis with both methods (Figure 4A).

#### 246 **Application: Maize infection with a bacterial pathogen**

247 Many economically important plant pathogens colonize the leaf apoplast at some point  
248 in the infection cycle, and a characteristic symptom of apoplast colonization is water-soaking.  
249 *Pnss*, which is the causal agent of Stewart's wilt disease in maize, produces strong water-  
250 soaking symptoms early after its colonization of the maize apoplast. This apoplast extraction  
251 method has facilitated the quantification of this symptom in infected and control plants (Figure  
252 4A). While apoplast hydration of untreated plants was ~20%, the apoplast hydration of buffer-  
253 infiltrated and infected plants was ~30% and ~60%, respectively, at the presymptomatic time  
254 point of 7 hours after infiltration (hai). Notably, each of these three levels of apoplast hydration  
255 differed significantly, whether calculated by the full or the abbreviated (percentage of weight  
256 increase) method. Also, the percentage of increase calculated by each of these methods did  
257 not differ significantly for any of the three sample types.

258 The isolation of microbes from an infected leaf is potentially of great use. The apoplast  
259 extracts obtained from *P. stewartii*-infected plants contain a visible bacterial fraction (Figure  
260 4B). To determine the efficiency of pathogen removal from the leaf during the extraction  
261 procedure, *P. stewartii* levels were assessed at 12 hai in both the apoplast extract and the  
262 remaining leaf tissue. From two biological replicates (n=4 for both isolated apoplast and  
263 remaining leaf samples), it was determined that 82% of the viable bacteria were present in the  
264 apoplast extract (Figure 4C). Thus, for infection systems where apoplast-localized microbes are  
265 efficiently isolated along with the apoplast fluid, this method will also be useful for subsequent

266 analysis of those microbes immediately following their isolation from the apoplast. We  
267 anticipate this method will be particularly useful for bacterial gene expression studies, as  
268 apoplast bacteria could be centrifuged directly into an RNA-protecting solution, thus “freezing”  
269 the bacterial transcriptome while effectively separating the bacteria from RNA-rich plant  
270 tissues.

### 271 **Discussion and Conclusion:**

272 The apoplast, while a physiologically important compartment of the plant leaf, is not  
273 often studied due to the difficulty of examining its contents without disrupting the surrounding  
274 tissue. One method that has facilitated study of the apoplast is the infiltration-centrifugation  
275 technique. While extraction of apoplast contents can be limited by the properties of the  
276 apoplast wash solution, this general method has nonetheless proven useful for the study of  
277 proteins, metabolites, and microorganisms localized in the apoplast.

278 To assess cytosolic contamination of apoplast extracts, activity of cellular enzymes such  
279 as malate dehydrogenase or glucose-6-phosphate dehydrogenase is often determined on a  
280 portion of the extract (Rico and Preston, 2008; O'Leary et al., 2016). Because of our small  
281 sample size (100  $\mu$ L or less per eight-leaf extraction), we used more sensitive, nonenzymatic  
282 tests to confirm that cellular integrity was not disrupted by the apoplast isolation procedure.  
283 Conductivity of ions as well as confocal microscopy of propidium iodide-stained cells indicate  
284 that we can obtain high-purity apoplast extracts from maize seedling leaves using this  
285 optimized infiltration-centrifugation technique. These tests were further confirmed by  
286 metabolite analysis, which revealed that apoplasts from untreated leaves contained less than  
287 1% of the total leaf phosphorylated compounds (unpublished data).

288 Another hallmark of the infiltration-centrifugation technique has been to determine the  
289 amount of liquid and/or air space in the apoplast. For example, the volume of liquid in the  
290 apoplast has been calculated by infiltrating the apoplast with a solution containing indigo  
291 carmine and comparing the extract's absorbance at 610 nm to a standard curve (Solomon and  
292 Oliver, 2001; O'Leary et al., 2016). However, potential technical issues exist with this method  
293 for some systems depending on the amount of silicon accumulation in the apoplast of the  
294 sampled leaf, which is especially common in monocots (Guerriero, et al., 2016). Indigo carmine,  
295 which is deep blue, can be cleaved into colorless products in the presence of silicon dioxide  
296 (silica) (Cao et al., 2016). This reaction ultimately dilutes the color of the indigo carmine, which  
297 in this application would suggest artificially high leaf apoplast hydration. Indeed, in our system  
298 with maize seedlings, the indigo carmine assay predicted only a 50% extraction efficiency of  
299 apoplast liquid contrary to our conclusive results in Figure 2B. As another method example, the  
300 nonaqueous air portion of the apoplast was determined by infiltrating the leaf with silicone  
301 fluid (Solomon and Oliver, 2001). In this study, we provide a method that directly measures  
302 both apoplast liquid volume and air space – and thus apoplast hydration – using calculations  
303 derived from leaf weights before, during, and after the procedure. As a further advantage,  
304 rather than representative samples, our method simply determines the apoplast hydration of  
305 every sample.

306 Utilizing this apoplast extraction method, we quantified the water-soaking response of  
307 plants infected with the bacterial pathogen *Pnss*. In the course of extracting the aqueous  
308 apoplast contents, we recovered a significant portion of apoplast-localized pathogen. The ease  
309 with which apoplast hydration can be assessed, as well as the ability to recover microbes from

310 the apoplast, will facilitate further study on many plant stress responses, including plant-  
311 pathogen interactions.

## 312 **Materials and Methods:**

### 313 **Maize growth conditions**

314 B73 maize (*Zea mays*) seedlings were grown in a Conviron growth chamber set to 30°C with an  
315 18-hour-light /6-hour-dark cycle. Ten to twelve seeds were planted per round 4-inch pot with  
316 MetroMix soil and watered every 36-48 hours or as needed. One to four hours prior to  
317 vacuum-infiltration treatments, which are independent of the apoplast isolation procedure,  
318 plants were watered and humidity elevated to > 65%.

### 319 **Bacteria growth conditions**

320 *Pantoea stewartii* subsp. *stewartii* (*Pnss*) wild-type strain DC283 (Coplin et al., 1986) was grown  
321 in LB broth with nalidixic acid (20 µg/mL) selection.

### 322 **Vacuum infiltration of maize seedlings**

323 Six-day-old B73 maize seedlings were vacuum-infiltrated with buffer or bacterial inoculum as  
324 described in (Asselin et al., 2015). Briefly, plants were inverted into a beaker with 300 mL 10  
325 mM KPO<sub>4</sub> buffer (control), *Pnss* at 10<sup>9</sup> CFU/mL, or 5% DMSO (Fisher Chemical D128-500), each  
326 containing 0.2% Tween-40 to facilitate infiltration. Using a Nalgene vacuum chamber, up to  
327 three pots at a time were subjected to a vacuum of 500 mmHg for 5 minutes, followed by  
328 vacuum release. The vacuum treatment was repeated two more times for a total of 15  
329 minutes. Plants were then allowed to air dry for 10-15 minutes until their return to the growth  
330 chamber with relative humidity at 65-70%.

### 331 **Confocal microscopy**

332 Maize seedlings were vacuum-infiltrated with buffer or 5% DMSO as described above. At 12  
333 hai, 1-cm segments of first-true-leaf tips were collected and stained in 100 µg/mL propidium  
334 iodide (Invitrogen #P3566 diluted in ddH<sub>2</sub>O) for 1 hour on ice and protected from light. With  
335 the adaxial side up, each leaf tip was mounted in water and sealed with a #1.5 coverslip and  
336 nail polish. Using a Nikon A1+ confocal microscope with 20x objective (numerical aperture  
337 0.75) and 1x confocal zoom, PI-stained cells were visualized by exciting leaves with a 561-nm  
338 laser and collecting emitted fluorescence at 605 nm. Images were acquired with Nikon NIS-  
339 Elements v4.20 software and further processed in Microsoft PowerPoint. For stained nuclei  
340 quantification, only cells with completely visible boundaries were counted.

#### 341 **Apoplast and *in planta* bacteria enumeration**

342 Six-day-old seedlings were vacuum infiltrated as described above with buffer or *Pnss*. At 12  
343 hours after infiltration, eight first true leaf tips were harvested from each treatment, leaf  
344 margins traced onto paper for subsequent determination of total leaf area, and apoplast  
345 extracted using sterile ddH<sub>2</sub>O. After apoplast extraction by centrifugation at 4°C for 10 minutes  
346 at 2,500 x g, leaves were placed on ice and apoplast extracts were resuspended and transferred  
347 to 1.5-mL microcentrifuge tubes to repellet the bacteria. Photos of apoplasts isolated from  
348 leaves infiltrated with WT bacteria or buffer and from untouched leaves (Figure 4B) were then  
349 taken for comparison. Next, the apoplast with WT bacteria was resuspended in cold ddH<sub>2</sub>O,  
350 serially diluted in septuplicate, and plated on LB solid media with nalidixic acid selection. Two  
351 1-cm disks were removed from each leaf with a cork borer, placed in 1 mL cold ddH<sub>2</sub>O,  
352 homogenized with 5-mm glass beads in a Qiagen TissueLyser for 1 minute at 30 Hz, serial  
353 diluted in triplicate, and plated on LB solid media with nalidixic acid selection. Plates were

354 incubated for 48 hours at room temperature before determining colony counts. Colony counts  
355 from leaf disc samples were converted to total colonies per sample based on the total area of  
356 the leaves, which was calculated by processing scanned images of the leaf traces with ImageJ  
357 software (<https://imagej.nih.gov/ij/>).

### 358 **Conductivity**

359 To assess conductivity from leaves before or after centrifugation, leaves were submerged in 30  
360 mL ddH<sub>2</sub>O for 1 hour with occasional gentle agitation. Leaves were then carefully removed and  
361 conductivity of the water measured with a WTW Cond 330i meter and TetraCon 325 probe.  
362 Blank water conductivity values were subtracted and then the resulting values were normalized  
363 to the initial leaf weight prior to syringe infiltration. Averages were obtained from three  
364 independent measurements.

365

### 366 **Acknowledgements:**

367 We would like to thank Dr. Anna Dobritsa of The Ohio State University for generously allowing  
368 our use of her Nikon A1+ confocal microscope. We also would like to thank our funding  
369 sources: Irene Gentzel was supported by the Translational Plant Sciences Graduate Program at  
370 The Ohio State University and by a USDA NIFA AFRI-ELI Predoctoral Fellowship (Award #  
371 20176701126080). The Mackey lab was supported by the US Department of Agriculture  
372 (National Institute of Food and Agriculture, grant #2015-11870612), and the Korean Rural  
373 Development Administration Next-Generation BioGreen 21 Program (System and Synthetic  
374 Agro-Biotech Center, PJ01326904). The Mackey and Alonso labs were supported by the Center  
375 for Applied Plant Sciences at The Ohio State University.

376 **Figure legends**

377 **Figure 1.** General procedure of maize leaf apoplast extraction. (A) First-true-leaf tips are  
378 harvested and syringe-infiltrated with the apoplast wash fluid. (B) The fully saturated leaves  
379 are wiped dry on their surface and placed on a 5x10 cm piece of Parafilm. A 1mL pipet tip is  
380 oriented in the opposite orientation as the leaves. (C) Keeping the leaves snug against the pipet  
381 tip, they are carefully wrapped into a cylinder. (D) To keep the bundle assembled, a second  
382 piece of Parafilm is wrapped around the leaves before inserting the bundle into a 15mL conical  
383 tube (E). The Parafilm is folded over the top of the tube before replacing the cap (F). The tube  
384 is then spun at 2,500 x g for 10 minutes at 4°C. After this step, the aqueous apoplast contents  
385 can be recovered separately from the intact leaf bundle (G). Although the leaf bundle often  
386 slides downwards during centrifugation, the size of the pipet tip ensures the bundle remains  
387 elevated above the liquid extract.

388 **Figure 2.** Evaluation of cellular integrity after apoplast extraction. (A) Conductivity of maize  
389 seedling leaves syringe-infiltrated with deionized water, 20% methanol, and 40% methanol.  
390 Error bars represent standard deviation of three replicates per treatment. Letters signify the  
391 significance between treatments, as assessed by one-way ANOVA followed by Tukey's HSD test  
392 where  $p \leq 0.05$ . (B) Impact of centrifugal force on the isolation of apoplast fluid from maize  
393 seedling leaves. Infiltrate represents the average volume syringe-infiltrated across all  
394 treatments. Conductivity of leaves was assessed after centrifugation. Error bars represent the  
395 standard deviation from three replicates for each treatment. (C) Representative photos of  
396 maize seedling leaf symptoms at 12 hours after vacuum-infiltration (hai) with buffer or 5%  
397 DMSO. (D) Confocal microscopic images of propidium iodide stained epidermal and mesophyll

398 cell layers of maize leaves at 12 hai with buffer or 5% DMSO. Shown are leaves that were not  
399 (top images) or were (bottom images) subjected to the apoplast extraction procedure. Two  
400 biological replicates, each with two samples per treatment, were analyzed. Scale bars are 100  
401  $\mu\text{m}$ .

402 **Figure 3.** Apoplast hydration calculation. (A) Apoplast hydration can be determined using leaf  
403 weights measured during the apoplast extraction procedure. (B) Apoplast hydration also  
404 determines the percent weight increase of leaves after the syringe-infiltration step. (C) Linear  
405 correlation between apoplast hydration calculated as in (A) and percent weight increase of  
406 syringe infiltrated leaves calculated as in (B), where  $n=130$ .

407 **Figure 4.** Application of the apoplast extraction method with a maize pathogen. (A) Apoplast  
408 hydration of maize leaves 7hai with wild-type *P. stewartii* or buffer, or leaves that were not  
409 previously infiltrated. Hydration determined with the calculated vs estimated methods yield  
410 non-significantly different values across treatments that are themselves significantly different.  
411 Significance between methods was assessed via t-test where  $p \leq 0.05$ , and significance between  
412 treatments was assessed via one-way ANOVA followed by Tukey's HSD test where  $p \leq 0.05$ . (B)  
413 Representative photos of apoplast extracts isolated from *P. stewartii*- or buffer-infiltrated  
414 plants at 12 hai compared to non-infiltrated plants. Note the large bacterial pellet in the *P.*  
415 *stewartii* extract. (C) Distribution of *P. stewartii* between the apoplast extract and the  
416 corresponding leaf tissue following apoplast extraction. Error bars represent standard  
417 deviation from two biological replicates where  $n=4$ .

418

## Parsed Citations

**Asselin JA, Lin J, Perez-Quintero AL, Gentzel I, Majerczak D, Opiyo SO, Zhao W, Paek SM, Kim MG, Coplin DL, Blakeslee JJ, Mackey D (2015) Perturbation of maize phenylpropanoid metabolism by an AvrE family type III effector from *Pantoea stewartii*. *Plant Physiol* 167: 1117-1135**

Pubmed: [Author and Title](#)

Google Scholar: [Author Only](#) [Title Only](#) [Author and Title](#)

**Beattie GA (2011) Water relations in the interaction of foliar bacterial pathogens with plants. *Annu Rev Phytopathol* 49: 533-555**

Pubmed: [Author and Title](#)

Google Scholar: [Author Only](#) [Title Only](#) [Author and Title](#)

**Bonfig KB, Gabler A, Simon UK, Luschin-Ebengreuth N, Hatz M, Berger S, Muhammad N, Zeier J, Sinha AK, Roitsch T (2010) Post-translational derepression of invertase activity in source leaves via down-regulation of invertase inhibitor expression is part of the plant defense response. *Mol Plant* 3: 1037-1048**

Pubmed: [Author and Title](#)

Google Scholar: [Author Only](#) [Title Only](#) [Author and Title](#)

**Cao Y, Gu X, Yu H, Zeng W, Liu X, Jiang S, Li Y (2016) Degradation of organic dyes by Si/SiO<sub>x</sub> core-shell nanowires: Spontaneous generation of superoxides without light irradiation. *Chemosphere* 144: 836-841**

Pubmed: [Author and Title](#)

Google Scholar: [Author Only](#) [Title Only](#) [Author and Title](#)

**Coplin DL, Frederick RD, Majerczak DR, Haas ES (1986) Molecular cloning of virulence genes from *Erwinia stewartii*. *J Bacteriol* 168: 619-623**

Pubmed: [Author and Title](#)

Google Scholar: [Author Only](#) [Title Only](#) [Author and Title](#)

**Coskun D, Deshmukh R, Sonah H, Menzies J, Reynolds O, Ma JF, Kronzucker HJ, Belanger RR (2018) The controversies of silicon's role in plant biology. *New Phytologist***

Pubmed: [Author and Title](#)

Google Scholar: [Author Only](#) [Title Only](#) [Author and Title](#)

**Cox KL, Meng F, Wilkins KE, Li F, Wang P, Booher NJ, Carpenter SCD, Chen LQ, Zheng H, Gao X, Zheng Y, Fei Z, Yu JZ, Isakeit T, Wheeler T, Frommer WB, He P, Bogdanove AJ, Shan L (2017) TAL effector driven induction of a SWEET gene confers susceptibility to bacterial blight of cotton. *Nat Commun* 8: 15588**

Pubmed: [Author and Title](#)

Google Scholar: [Author Only](#) [Title Only](#) [Author and Title](#)

**Delmer DP (1979) Dimethylsulfoxide as a potential tool for analysis of compartmentation in living plant cells. *Plant Physiol* 64: 623-629**

Pubmed: [Author and Title](#)

Google Scholar: [Author Only](#) [Title Only](#) [Author and Title](#)

**Floerl S, Majcherczyk A, Possienke M, Feussner K, Tappe H, Gatz C, Feussner I, Kües U, Polle A (2012) *Verticillium longisporum* infection affects the leaf apoplastic proteome, metabolome, and cell wall properties in *Arabidopsis thaliana*. *PLoS One* 7: e31435**

Pubmed: [Author and Title](#)

Google Scholar: [Author Only](#) [Title Only](#) [Author and Title](#)

**Führs H, Götze S, Specht A, Erban A, Gallien S, Heintz D, Van Dorsselaer A, Kopka J, Braun HP, Horst WJ (2009) Characterization of leaf apoplastic peroxidases and metabolites in *Vigna unguiculata* in response to toxic manganese supply and silicon. *J Exp Bot* 60: 1663-1678**

Pubmed: [Author and Title](#)

Google Scholar: [Author Only](#) [Title Only](#) [Author and Title](#)

**Geiger DR, Sovonick SA, Shock TL, Fellows RJ (1974) Role of free space in translocation in sugar beet. *Plant Physiol* 54: 892-898**

Pubmed: [Author and Title](#)

Google Scholar: [Author Only](#) [Title Only](#) [Author and Title](#)

**Geilfus CM (2017) The pH of the Apoplast: Dynamic Factor with Functional Impact Under Stress. *Mol Plant* 10: 1371-1386**

Pubmed: [Author and Title](#)

Google Scholar: [Author Only](#) [Title Only](#) [Author and Title](#)

**Giaquinta R (1977) Phloem Loading of Sucrose: pH Dependence and Selectivity. *Plant Physiol* 59: 750-755**

Pubmed: [Author and Title](#)

Google Scholar: [Author Only](#) [Title Only](#) [Author and Title](#)

**Guerrero G, Hausman JF, Legay S (2016) Silicon and the Plant Extracellular Matrix. *Front Plant Sci* 7: 463**

Pubmed: [Author and Title](#)

Google Scholar: [Author Only](#) [Title Only](#) [Author and Title](#)

**Jia W, Davies WJ (2007) Modification of leaf apoplastic pH in relation to stomatal sensitivity to root-sourced abscisic acid signals. *Plant Physiol* 143: 68-77**

Pubmed: [Author and Title](#)

Google Scholar: [Author Only](#) [Title Only](#) [Author and Title](#)

Jones JD, Dangl JL (2006) The plant immune system. *Nature* 444: 323-329

Pubmed: [Author and Title](#)

Google Scholar: [Author Only](#) [Title Only](#) [Author and Title](#)

Jones K, Kim DW, Park JS, Khang CH (2016) Live-cell fluorescence imaging to investigate the dynamics of plant cell death during infection by the rice blast fungus *Magnaporthe oryzae*. *BMC Plant Biol* 16: 69

Pubmed: [Author and Title](#)

Google Scholar: [Author Only](#) [Title Only](#) [Author and Title](#)

Joosten MH (2012) Isolation of apoplastic fluid from leaf tissue by the vacuum infiltration-centrifugation technique. *Methods Mol Biol* 835: 603-610

Pubmed: [Author and Title](#)

Google Scholar: [Author Only](#) [Title Only](#) [Author and Title](#)

Kandel SL, Joubert PM, Doty SL (2017) Bacterial Endophyte Colonization and Distribution within Plants. *Microorganisms* 5

Pubmed: [Author and Title](#)

Google Scholar: [Author Only](#) [Title Only](#) [Author and Title](#)

Koch W, Kwart M, Laubner M, Heineke D, Stransky H, Frommer WB, Tegeder M (2003) Reduced amino acid content in transgenic potato tubers due to antisense inhibition of the leaf H<sup>+</sup>/amino acid symporter StAAP1. *Plant J* 33: 211-220

Pubmed: [Author and Title](#)

Google Scholar: [Author Only](#) [Title Only](#) [Author and Title](#)

Kwon C, Bednarek P, Schulze-Lefert P (2008) Secretory pathways in plant immune responses. *Plant Physiol* 147: 1575-1583

Pubmed: [Author and Title](#)

Google Scholar: [Author Only](#) [Title Only](#) [Author and Title](#)

Lalonde S, Tegeder M, Throne-Holst M, Frommer WB, Patrick JW (2003) Phloem loading and unloading of sugars and amino acids. *Plant, Cell, and Environment* 26: 37-56

Pubmed: [Author and Title](#)

Google Scholar: [Author Only](#) [Title Only](#) [Author and Title](#)

Lawson T, Simkin AJ, Kelly G, Granot D (2014) Mesophyll photosynthesis and guard cell metabolism impacts on stomatal behaviour. *New Phytol* 203: 1064-1081

Pubmed: [Author and Title](#)

Google Scholar: [Author Only](#) [Title Only](#) [Author and Title](#)

Liu H, Carvalhais LC, Crawford M, Singh E, Dennis PG, Pieterse CMJ, Schenk PM (2017) Inner Plant Values: Diversity, Colonization and Benefits from Endophytic Bacteria. *Front Microbiol* 8: 2552

Pubmed: [Author and Title](#)

Google Scholar: [Author Only](#) [Title Only](#) [Author and Title](#)

Liu Q, Luo L, Zheng L (2018) Lignins: Biosynthesis and Biological Functions in Plants. *Int J Mol Sci* 19

Pubmed: [Author and Title](#)

Google Scholar: [Author Only](#) [Title Only](#) [Author and Title](#)

Lohaus G, Pennewiss K, Sattelmacher B, Hussmann M, Hermann Muehling K (2001) Is the infiltration-centrifugation technique appropriate for the isolation of apoplastic fluid? A critical evaluation with different plant species. *Physiol Plant* 111: 457-465

Pubmed: [Author and Title](#)

Google Scholar: [Author Only](#) [Title Only](#) [Author and Title](#)

López-Millán AF, Morales F, Abadía A, Abadía J (2000) Effects of iron deficiency on the composition of the leaf apoplastic fluid and xylem sap in sugar beet. Implications for iron and carbon transport. *Plant Physiol* 124: 873-884

Pubmed: [Author and Title](#)

Google Scholar: [Author Only](#) [Title Only](#) [Author and Title](#)

Naseem M, Kunz M, Dandekar T (2017) Plant-Pathogen Maneuvering over Apoplastic Sugars. *Trends Plant Sci* 22: 740-743

Pubmed: [Author and Title](#)

Google Scholar: [Author Only](#) [Title Only](#) [Author and Title](#)

Notman R, Noro M, O'Malley B, Anwar J (2006) Molecular basis for dimethylsulfoxide (DMSO) action on lipid membranes. *J Am Chem Soc* 128: 13982-13983

Pubmed: [Author and Title](#)

Google Scholar: [Author Only](#) [Title Only](#) [Author and Title](#)

Nouchi I, Hayashi K, Hiradate S, Ishikawa S, Fukuoka M, Chen CP, Kobayashi K (2012) Overcoming the difficulties in collecting apoplastic fluid from rice leaves by the infiltration-centrifugation method. *Plant Cell Physiol* 53: 1659-1668

Pubmed: [Author and Title](#)

Google Scholar: [Author Only](#) [Title Only](#) [Author and Title](#)

O'Leary BM, Neale HC, Geilfus CM, Jackson RW, Arnold DL, Preston GM (2016) Early changes in apoplast composition associated with defence and disease in interactions between *Phaseolus vulgaris* and the halo blight pathogen *Pseudomonas syringae* Pv. phaseolicola. *Plant Cell Environ* 39: 2172-2184

Pubmed: [Author and Title](#)

Google Scholar: [Author Only](#) [Title Only](#) [Author and Title](#)

**O'Leary BM, Rico A, McCraw S, Fones HN, Preston GM (2014) The infiltration-centrifugation technique for extraction of apoplastic fluid from plant leaves using *Phaseolus vulgaris* as an example. *J Vis Exp***

Pubmed: [Author and Title](#)

Google Scholar: [Author Only](#) [Title Only](#) [Author and Title](#)

**Rasoolizadeh A, Labbé C, Sonah H, Deshmukh RK, Belzile F, Menzies JG, Bélanger RR (2018) Silicon protects soybean plants against *Phytophthora sojae* by interfering with effector-receptor expression. *BMC Plant Biol* 18: 97**

Pubmed: [Author and Title](#)

Google Scholar: [Author Only](#) [Title Only](#) [Author and Title](#)

**Rico A, Preston GM (2008) *Pseudomonas syringae* pv. tomato DC3000 uses constitutive and apoplast-induced nutrient assimilation pathways to catabolize nutrients that are abundant in the tomato apoplast. *Mol Plant Microbe Interact* 21: 269-282**

Pubmed: [Author and Title](#)

Google Scholar: [Author Only](#) [Title Only](#) [Author and Title](#)

**Rottmann TM, Fritz C, Lauter A, Schneider S, Fischer C, Danzberger N, Dietrich P, Sauer N, Stadler R (2018) Protoplast-Esculin Assay as a New Method to Assay Plant Sucrose Transporters: Characterization of AtSUC6 and AtSUC7 Sucrose Uptake Activity in Arabidopsis Col-0 Ecotype. *Front Plant Sci* 9: 430**

Pubmed: [Author and Title](#)

Google Scholar: [Author Only](#) [Title Only](#) [Author and Title](#)

**Sattelmacher B (2000) The apoplast and its significance for plant mineral nutrition. *New Phytologist* 149: 167-192**

Pubmed: [Author and Title](#)

Google Scholar: [Author Only](#) [Title Only](#) [Author and Title](#)

**Schwartz AR, Morbitzer R, Lahaye T, Staskawicz BJ (2017) TALE-induced bHLH transcription factors that activate a pectate lyase contribute to water soaking in bacterial spot of tomato. *Proc Natl Acad Sci U S A* 114: E897-E903**

Pubmed: [Author and Title](#)

Google Scholar: [Author Only](#) [Title Only](#) [Author and Title](#)

**Solomon PS, Oliver RP (2001) The nitrogen content of the tomato leaf apoplast increases during infection by *Cladosporium fulvum*. *Planta* 213: 241-249**

Pubmed: [Author and Title](#)

Google Scholar: [Author Only](#) [Title Only](#) [Author and Title](#)

**Veillet F, Gaillard C, Coutos-Thévenot P, La Camera S (2016) Targeting the AtCWN1 gene to explore the role of invertases in sucrose transport in roots and during *Botrytis cinerea* infection. *Front Plant Sci* 7: 1899**

Pubmed: [Author and Title](#)

Google Scholar: [Author Only](#) [Title Only](#) [Author and Title](#)

**Wang L, Cai K, Chen Y, Wang G (2013) Silicon-mediated tomato resistance against *Ralstonia solanacearum* is associated with modification of soil microbial community structure and activity. *Biol Trace Elem Res* 152: 275-283**

Pubmed: [Author and Title](#)

Google Scholar: [Author Only](#) [Title Only](#) [Author and Title](#)

**Wang M, Gao L, Dong S, Sun Y, Shen Q, Guo S (2017) Role of Silicon on Plant-Pathogen Interactions. *Front Plant Sci* 8: 701**

Pubmed: [Author and Title](#)

Google Scholar: [Author Only](#) [Title Only](#) [Author and Title](#)

**Wang Y, Kang Y, Ma C, Miao R, Wu C, Long Y, Ge T, Wu Z, Hou X, Zhang J, Qi Z (2017) CNGC2 Is a Ca<sup>2+</sup> Influx Channel That Prevents Accumulation of Apoplastic Ca<sup>2+</sup> in the Leaf. *Plant Physiol* 173: 1342-1354**

Pubmed: [Author and Title](#)

Google Scholar: [Author Only](#) [Title Only](#) [Author and Title](#)

**Witzel K, Shahzad M, Matros A, Mock HP, Mühling KH (2011) Comparative evaluation of extraction methods for apoplastic proteins from maize leaves. *Plant Methods* 7: 48**

Pubmed: [Author and Title](#)

Google Scholar: [Author Only](#) [Title Only](#) [Author and Title](#)

**Wright CA, Beattie GA (2004) *Pseudomonas syringae* pv. tomato cells encounter inhibitory levels of water stress during the hypersensitive response of *Arabidopsis thaliana*. *Proc Natl Acad Sci U S A* 101: 3269-3274**

Pubmed: [Author and Title](#)

Google Scholar: [Author Only](#) [Title Only](#) [Author and Title](#)

**Xin XF, Nomura K, Aung K, Velásquez AC, Yao J, Boutrot F, Chang JH, Zipfel C, He SY (2016) Bacteria establish an aqueous living space in plants crucial for virulence. *Nature* 539: 524-529**

Pubmed: [Author and Title](#)

Google Scholar: [Author Only](#) [Title Only](#) [Author and Title](#)

**Yamada K, Saijo Y, Nakagami H, Takano Y (2016) Regulation of sugar transporter activity for antibacterial defense in *Arabidopsis*. *Science* 354: 1427-1430**

Pubmed: [Author and Title](#)

Google Scholar: [Author Only](#) [Title Only](#) [Author and Title](#)

**Zhang C, Turgeon R (2018) Mechanisms of phloem loading. Curr Opin Plant Biol 43: 71-75**

Pubmed: [Author and Title](#)

Google Scholar: [Author Only](#) [Title Only](#) [Author and Title](#)